Energy Management of a Hybrid Electric Vehicle

Ahmed Khadhraoui
Analysis and Treatment of Electrical and Energy Signals
and Systems (ATSSEE) Laboratory
Faculty of Sciences of Tunis
Tunis El-Manar University, Tunisia
ahmed.khadhraoui@fst.utm.tn

Tarek Selmi
Analysis and Treatment of Electrical and Energy Signals
and Systems (ATSSEE) Laboratory
Faculty of Sciences of Tunis
Tunis El-Manar University, Tunisia
t.selmi@issatkr.u-kairouan.tn

Adnen Cherif
Analysis and Treatment of Electrical and Energy Signals and Systems (ATSSEE) Laboratory
Faculty of Sciences of Tunis
Tunis El-Manar University, Tunisia
Adnen2fr@yahoo.fr

Abstract-Electric Vehicles (EVs) are becoming more popular and gaining attention due to a combination of factors such as falling prices and increasing environmental awareness. EVs fall into several categories related to energy production and storage. Standard developed, tested, and commercialized EV technologies include Fuel Cell Electric Vehicles (FCEVs), All Electric Vehicles (AEVs), also known as Battery Electric Vehicles (BEVs), Plug-in Hybrid Electric Vehicles (PHEVs), Hybrid Electric Vehicles (HEVs), and Flexible Fuel Vehicles (FFVs). Still, the advantages of FCEVs are relatively small compared to other autonomous and refueling technologies. Considering the above aspects, this work presents a Matlab/Simulink model of an FCEV's behavior and opportunities.

Keywords-fuel cell; electric vehicle; EMS; solar energy; PEM; Matlab; dynamic-modeling

I. INTRODUCTION

Nowadays, the gases emitted by fossil fuel-based vehicles are seriously threatening the environment and directly impact climate [1, 2]. Global warming and climate change are amplified by pollution due to the extensive burn of diesel by diesel-based vehicles [3, 4]. It has been reported that transportation is the origin of 24% of CO_2 emissions worldwide [5]. Even worse, in 2020, the European Environment Agency suggested that about 27% of CO_2 is emitted by the transport sector, while more than 70% of emissions are mainly caused by vehicles [5]. From the 1970s, fossil fuel combustion increased the emission of CO_2, CO, SO_2, and NO by 90% to reach 36.1Gt in 2014 [6]. For this reason the petroleum cars represent one of the most important sources of pollution to the environment [7]. Moreover, this type of car is witnessing an increasing demand from citizens. With this development, research and studies on clean energy have multiplied. These factors, aim to reduce pollution and encourage people to use Electric Vehicles (EVs) [8].

The standard EV utilizes one energy source, however it is not profitable in return. So, it has been upgraded by adding a second source with an Energy Management System (EMS). The complex setup and behavior of the multi-source hybrid power system puts additional requirements on the operation of the EMS. Regardless of the design of the power system, the EMS manages the power flow of the transducer in real time to achieve the control goal [9]. Therefore, the optimal control algorithm used in the driving cycle can be used as a representative research program for energy management technology.

EMS was selected as a potential research problem in industry and academia [10]. In the evaluation of the existing literature, there are many classifications of energy management methods. EMSs are classified into three types according to their optimization strategy: rule-based, local, and global. In [11], the authors outline the EMS of plug-in hybrid EVs. The classification of energy management is discussed, including rule-based and optimization-based control systems. In [12], the authors compare the advantages and disadvantages of each technique. Finally, many aspects of real-time implementation (for example, computational burden and optimization) are discussed. In [13], the authors examine and show various classifications of hybrid EVs that use hydraulic drive-classifying and internet-related technologies. With the advancement of ITS technology and machine learning methods (such as adaptability and real-time execution) [14], a new EMS is being created to meet the increasing performance requirements. However, a complete evaluation of EMSs is needed to better grasp the current technology and future research work. Unlike previous EMS studies, this one includes a complex ranking system.

There are two types of offline EMS: one based on global improvement and one based on regulations [15]. Instant improvement, predictive improvement, and learning-based

---

Corresponding author: Ahmed Khadhraoui

improvement are three types of online environmental management systems [16]. Since the proposed technology contains various methods for solution goals, optimization, and real-time implementation, a thorough review of the literature is conducted. The concepts, advantages and disadvantages of each technology are compared, and the design and operational characteristics of the proposed scheme are highlighted [17]. Finally, the development of a new EMS and recent literature highlight the important prospects for macromolecules. The hybrid part on a vehicle is the application of two energy sources. The Proton Exchange Membrane Fuel Cell (PEMFC) [18] is the best type for the EV due to its high efficiency and fast response rate with back up source (super-capacitor (SC)) [19]. The addition of photovoltaic (PV) energy will reduce the consummation of hydrogen up to 40% [20].

The current article describes a realistic environmental management system for the PVFCEV. The proposed method was developed in response to various constraints, including energy requirements and subsystems. Unlike previous papers, it avoids clustering (on/off) and global/local optimization, which may be deceptive due to algorithm modification and implementation assumptions. Instead, each algorithm is presented and reviewed individually, emphasizing its advantages and limitations, as well as alternative technologies to compensate for them.

II. THE SYSTEM DESCRIPTION OF THE PVFCEV

The PVFCEV consists of a PEMFC stack, hydrogen tank, a Super-Capacitor (SC), a PV array as a secondary power source, EMS, and an electric motor with driveline. The model description is shown in Figure 1.
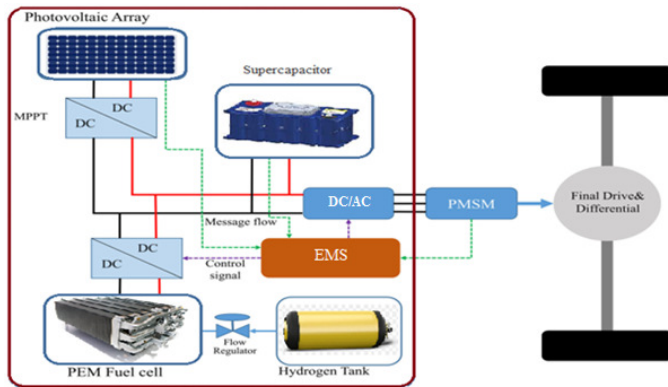

Fig. 1.   Schematic of the PVFCEV.

The FC system is the principal energy source. The details of the FC used on the Simulink model are shown in Table I.

TABLE I.   THE DETAILS OF THE FC

Parameter	Value
Number of cells	65
Nominal power	4.2 kW
Nominal voltage	45 V
Peak power	6 kW
Fuel supply pressure	1.5 bar

The SC has high power density and fast response. It gives power in the acceleration phase and is recharged by the excess energy generated by regenerative braking and the PV array. The main parameters of the SC source and the PV array are shown in Table II and III.

TABLE II.   SUPER-CAPACITOR MAIN PARAMETERS

Parameter	Value
Rated capacitance	15.6 F
Rated voltage	291 V
Initial voltage	270 V
Number of series capacitors	105
Current prior open circuit	10 A
SOC start	80%

TABLE III.   THE PARAMETERS OF THE PV ARRAY

Parameter	Value
Number of cells per module	72
Max power per module	250 W
Nominal voltage	50 V
Circuit current	6.3 A
Fuel supply pressure	1.5 bar
Number of series-connected module	2

The Permanent Magnet Synchronous Motor (PMSM) was chosen thanks to its high operating efficiency and reliability. The EMS monitors the working status of the system, including PV array power, SC SOC, and the required power, to determine the power of the FC and the torque of the motor. The vehicle is subjected to several forces, where some of their vectors lead to the traction force (Figure 2).
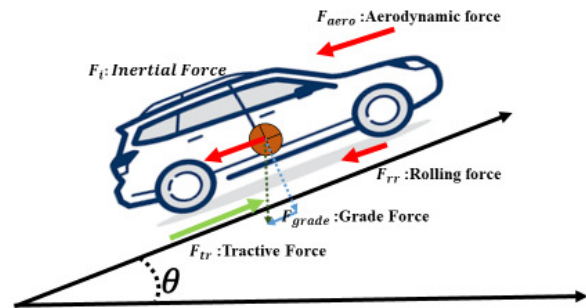

Fig. 2.   The ttractive forces on the vehicle.

The F_{Tr} traction force is needed to overcome the resistance to advance and accelerate the vehicle. It is written in the form of:

$$F_{tr} = F_{aero} + F_i + F_{arade} + F_{rr} \quad (1)$$

Thus, according to Newton's second law, the acceleration α can be expressed by.

$$\alpha = \frac{F_{tr} - (F_{aero} + F_{grade} + F_{rr})}{m_i} \quad (2)$$

F_{aero} is the aerodynamic force (N):

$$F_{aero} = \frac{1}{2}\rho C_d A_f V^2 \quad (3)$$

F_{rr} is the rolling force:

$$F_{rr} = mg C_{rr} \quad (4)$$

F_{grade} is the resistance force of hill climb:

$$F_{grade} = mg \sin(\theta) \quad (5)$$

Table IV shows the hybrid EV's parameters.

TABLE IV.   PARAMETERS OF THE VEHICLE

Parameter	Value
Vehicle mass	1400 Kg
Gravity	9.8 m/s^2
Air density	1.18 kg/m^3
Road angle	0.5 degrees
Air drag	0.38

III.   THE ENERGY MANAGEMENT SYSTEM

The EMS is based on the output of the SOC of the SC, the PV and the power demanded from the electric motor as shown in the figure 3.
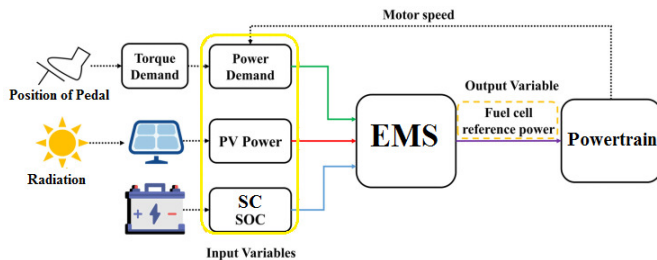

Fig. 3.   The scheme of the EMS: PV, FC, SC, and EV.

The position of the pedal determines the power needed from the motor. To determine the powers of the SC and the FC, the FC power is selected as the principal control variable of the controller. From Figure 3, the bus capacitive energy of EMS (E_{EMS}) is:

$$E_{EMS} = P_{FC} + P_{PV} + P_{SC} - P_{Ch} \quad (6)$$

The FC stack and the PV are generators (P_{Gen}):

$$P_{Gen} = P_{FC} + P_{PV} \quad (7)$$

By combination (6) and (7) we get:

$$E_{EMS} = P_{Gen} + P_{SC} - P_{Ch} \quad (8)$$

The generators' power is:

$$P_{Gen} = E_{EMS} - P_{SC} + P_{Ch} \quad (9)$$

General, the PV panel cannot be fast in terms of electricity production. For this case, the FC power compensates the lack of energy as given in (10):

$$P_{FC\_ref} = P_{Gen} - P_{PV} \quad (10)$$

Moreover, we made a fuzzy algorithm with 3 inputs (*cycle*, P_{PV}, and P_{SC}) and the output is the $P_{FC\ ref}$ as shown in Figure 4. Figures 4, 5, 6, and 7) represent the input and the output of the fuzzy algorithm according to 45 rules.

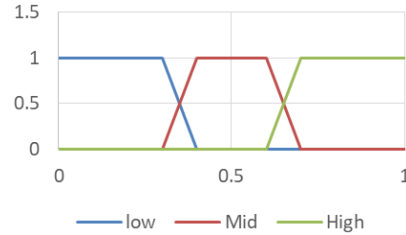

Fig. 4.   Input parameter PV.
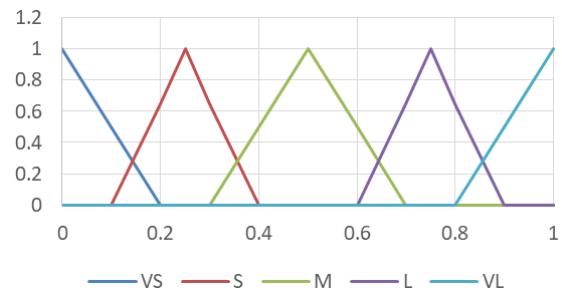

Fig. 5.   Input parameter SOC.

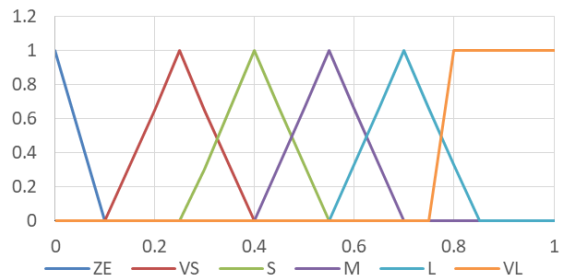Fig. 6.   Input parameter power demand.

Fig. 7.   Output parameter FC.

The pedal determines the power demanded for a specific torque. The pedal represents the brake and the accelerator. The pressure ratio on the pedal is present in the testing model in the simulation. In the fuzzy system, the power is between 0 and 1. The fuzzy set for the PV are low, middle, and high to represent the intensity of the solar radiation. The fuzzy set for the SOC of SC are low, middle, and high to represent the radio of the residual capacity. The power demand is split into five levels, from Very Small (VS) to Very Large (VL) after passing Small (S), Middle (Mid), and Large (L). Finally, the fuzzy set of the FC has 6 levels: Zero (ZE), VS, S, M, L, and VL. The rules of the fuzzy reasoning are presented in Table V. The algorithm was developed in Matlab.

The EM of the PV array is controlled by the Perturb and Observation (P&O) algorithm. Figure 8, presents the flowchart of the EMS algorithm for the PV. This method gives excellent results among different MPPT techniques.

TABLE V.   FUZZY REASONING RULES

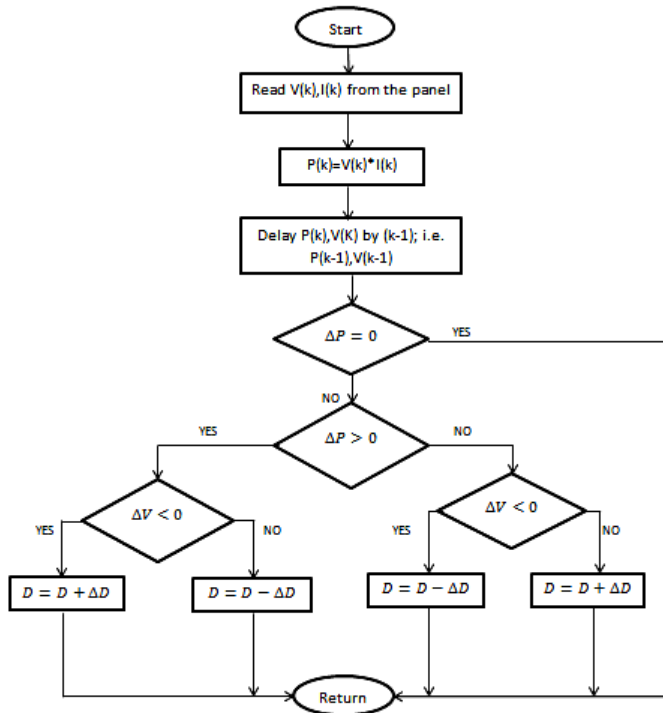| Inp SOC	Inp PV	Inp P_{Load}				
		VS	S	M	L	VL
Low	Low	VS	M	L	L	VL
Low	Middle	VS	S	M	L	VL
Low	High	VS	S	M	M	L
Middle	Low	ZE	VS	S	M	L
Middle	Middle	ZE	VS	S	M	M
Middle	High	ZE	ZE	VS	S	M
High	Low	ZE	ZE	VS	VS	S
High	Middle	ZE	ZE	ZE	VS	S
High	High	ZE	ZE	ZE	ZE	VS

Fig. 8.   Flowchart of the P&O algorithm.

IV. RESULTS AND DISCUSSION

In order to validate the proposed EMS, the PVFCEV mode was simulated in Matlab/Simulink. We started testing the model with the following cycle of pedal positions:

- Time ∈ [0. . .2s] stop: The pedal is at 0%

- Time ∈ [3s. . .6s] acceleration: The pedal is at 80%

- Time ∈ [7s . . . 17s] stability: the pedal is at 70%

- Time ∈ [18s . . . 27s] apply the brakes: the pedal is at 75 %

- Time ∈ [28s . . . 30s] system shutdown

Figure 9 shows the results of model under the following conditions: 500W/m^2 solar radiance, 25^{0}C temperature, and 80% SOC of the super-capacity. The SOC of the SC is high with medium radiation, the SC acts as the principal source on the [2s... 6s] period, according to the faster response of the SC compared to the FC. However, the SC is in the recharging mode during [0...2s] and when the vehicle stops. The power of

the SC during [0..2s] is negative and this action means that the PV array is charging the SC. The FC started to produce power at the 3rd second. When the FC power tries to become stable, the SC powers down and starts to recharge during [6...7s]. The period os [6s….7s] represents the change of acceleration from 80% to 70%.
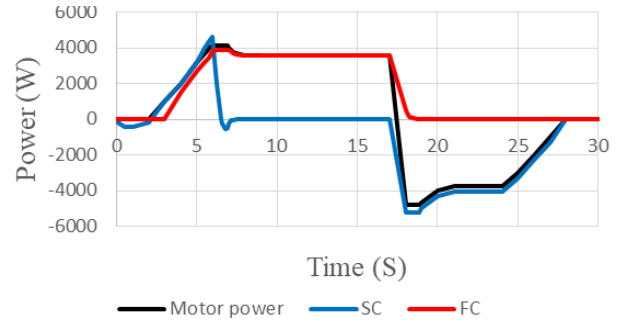

Fig. 9.   Simulation results of the vehicle for 500W/m^2 solar radiation.

The FC becomes the principal source in [8s…17s]. The FC power is the same as the motor power according to the stability of the system in that duration. After that, the FC power becomes zero and the power of the motor becomes negative due to the baking during [18s...27s]. At this time, the engine is trying as a primary source to recharge the SC. At the end, the vehicle stops and the power of the system is zero. The NEDC (New European Driving Cycle) is one of the cycles used to measure the degree of performance of the vehicle engines and energy economy. This cycle is divided in two parts: the first part is represented from 0s to 800s (urban driving cycle) and the second part from 800 s to 1200s (extra urban driving cycle) in Figure 10. The demand power (P_{Ch}) of the vehicle when the path traveled corresponds to the NEDC speed profile is given by Figure 11.

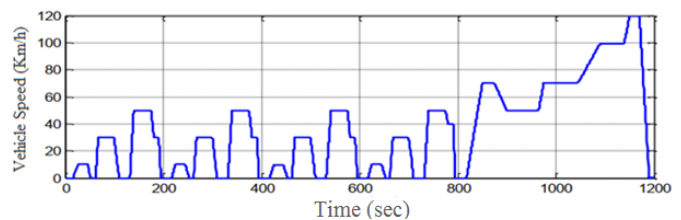$$P_{Ch} = P_{FC} + P_{PV} + P_{SC} \quad (11)$$

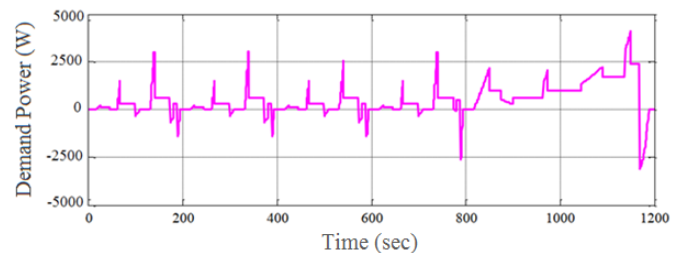Fig. 10.   Profile of vehicle speed (NEDC).

Fig. 11.   Demand power.

The power delivery of the vehicle (P_{ch}), the FC power, and the SC power are shown in Figure 12. We can see that the power profile of the FC depends on the fuzzy rules applied and the power profile requested. This allows meeting the demands of the vehicle while ensuring an energy exchange between the FC and SC during the traction phase, precisely, for the calls of low power and when the SOC of the SC has low values. In this case, the FC allows, at the same time, satisfying the demand of the vehicle and charging the pack of SCs. The gap between the power supplied by the FC and that required by the traction system is used to ensure the loading phase of the storage system. The SC load reached a high value during the FC stress period up to t = 965s. This is explained by the use of the SC during the braking phases most of the time. Thereafter, the SOC value decreases during the interval up to t=1170s when it is solicited from the FC. When the vehicle is in acceleration mode and the SC SOC is average, the SC shoulders the FC to provide the required power. The FC provides the power required charging the SC during the acceleration mode and when the SOC of the SC is low. In this case, the SC can easily recover from the braking energy.
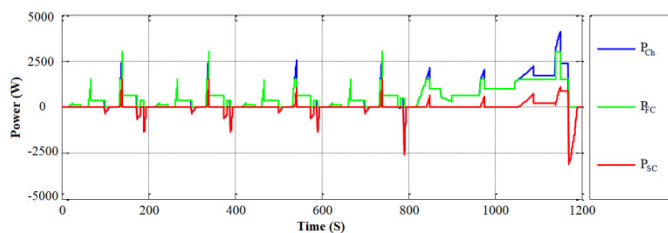

Fig. 12.   Power elements.

V.   CONCLUSIONS

This paper presents the technical results of PVFCEV via a mathematic model with a fuzzy algorithm designed for it. The EMS of the vehicle using the power of the PV, the demand power and the SOC of an SC as input parameters. The output of the EMS is the reference power of the FC. The use of the SC contributed to improving the vehicle's effectiveness in the acceleration phase, similar to previous research that remained in the use of the battery despite its poor efficacy. The EMS was validated by the simulation results. In order to get good results, the simulation started by the cycle of pedal position as a first step and the NEDC driving cycle was considered in the next phase. The proposed EMS operated efficiently and robustly under rapid changes in power demand, changes in solar power, and different levels of SC SOC.

In future work, we will focus on the design and implementation of experiments to validate the proposed PVFCHEV and its EMS. The PVFCEV physical model in this work helps to facilitate the design of the experimental setup, as real physical component models are used.

REFERENCES

[1]   M. A. Hannan, M. S. H. Lipu, A. Hussain, and A. Mohamed, "A review of lithium-ion battery state of charge estimation and management system in electric vehicle applications: Challenges and recommendations," *Renewable and Sustainable Energy Reviews*, vol. 78, pp. 834–854, Oct. 2017, https://doi.org/10.1016/j.rser.2017.05.001.

[2]   F. Hou *et al.*, "Comprehensive analysis method of determining global long-term GHG mitigation potential of passenger battery electric vehicles," *Journal of Cleaner Production*, vol. 289, Mar. 2021, Аρτ. No. 125137, https://doi.org/10.1016/j.jclepro.2020.125137.

[3]   M. S. H. Lipu *et al.*, "A review of state of health and remaining useful life estimation methods for lithium-ion battery in electric vehicles: Challenges and recommendations," *Journal of Cleaner Production*, vol. 205, pp. 115–133, Dec. 2018, https://doi.org/10.1016/j.jclepro.2018.09.065.

[4]   B. Ameyaw, L. Yao, A. Oppong, and J. K. Agyeman, "Investigating, forecasting and proposing emission mitigation pathways for CO2 emissions from fossil fuel combustion only: A case study of selected countries," *Energy Policy*, vol. 130, pp. 7–21, Jul. 2019, https://doi.org/10.1016/j.enpol.2019.03.056.

[5]   "Greenhouse gas emissions from transport in Europe," *European Environment Agency*. https://www.eea.europa.eu/data-and-maps/indicators/transport-emissions-of-greenhouse-gases (accessed Jun. 11, 2022).

[6]   M.-K. Tran *et al.*, "A Review of Range Extenders in Battery Electric Vehicles: Current Progress and Future Perspectives," *World Electric Vehicle Journal*, vol. 12, no. 2, Jun. 2021, Art. no. 54, https://doi.org/10.3390/wevj12020054.

[7]   A. Mansouri and T. Hafedh, "Torque Ripple Minimization and Performance Investigation of an In-Wheel Permanent Magnet Motor," *Engineering, Technology & Applied Science Research*, vol. 6, no. 3, pp. 987–992, Jun. 2016, https://doi.org/10.48084/etasr.644.

[8]   K. Y. Bjerkan, T. E. Nørbech, and M. E. Nordtømme, "Incentives for promoting Battery Electric Vehicle (BEV) adoption in Norway," *Transportation Research Part D: Transport and Environment*, vol. 43, pp. 169–180, Mar. 2016, https://doi.org/10.1016/j.trd.2015.12.002.

[9]   B. Zafar, S. Benslama, S. Nasri, and M. Mahmoud, "Smart Home Energy Management System Design: A Realistic Autonomous V2H / H2V Hybrid Energy Storage System," *International Journal of Advanced Computer Science and Applications*, vol. 10, no. 6, pp. 217–223, Jun. 2019.

[10]   K. Sharma, "Feature-based efficient vehicle tracking for a traffic surveillance system," *Computers & Electrical Engineering*, vol. 70, pp. 690–701, Aug. 2018, https://doi.org/10.1016/j.compeleceng.2017.10.002.

[11]   H. Eroğlu and Y. Oğuz, "Energy Efficient Driving Optimization of Electrical Vehicles Considering the Road Characteristics," *Balkan Journal of Electrical and Computer Engineering*, vol. 9, no. 2, pp. 161–170, Apr. 2021, https://doi.org/10.17694/bajece.902485.

[12]   B. Rajani and D. C. Sekhar, "A hybrid optimization based energy management between electric vehicle and electricity distribution system," *International Transactions on Electrical Energy Systems*, vol. 31, no. 6, 2021, Art. no. e12905, https://doi.org/10.1002/2050-7038.12905.

[13]   M. K. Gerritsma, T. A. AlSkaif, H. A. Fidder, and W. G. J. H. M. van Sark, "Flexibility of Electric Vehicle Demand: Analysis of Measured Charging Data and Simulation for the Future," *World Electric Vehicle Journal*, vol. 10, no. 1, Mar. 2019, Art. no 14, https://doi.org/10.3390/wevj10010014.

[14]   H. Ngo, A. Kumar, and S. Mishra, "Optimal positioning of dynamic wireless charging infrastructure in a road network for battery electric vehicles," *Transportation Research Part D: Transport and Environment*, vol. 85, Aug. 2020, Art. no. 102385, https://doi.org/10.1016/j.trd.2020.102385.

[15]   S. Khan, A. Ahmad, F. Ahmad, M. Shafaati Shemami, M. Saad Alam, and S. Khateeb, "A Comprehensive Review on Solar Powered Electric Vehicle Charging System," *Smart Science*, vol. 6, no. 1, pp. 54–79, Jan. 2018, https://doi.org/10.1080/23080477.2017.1419054.

[16]   M. E. Bendib and A. Mekias, "Solar Panel and Wireless Power Transmission System as a Smart Grid for Electric Vehicles," Engineering*, Technology & Applied Science Research*, vol. 10, no. 3, pp. 5683–5688, Jun. 2020, https://doi.org/10.48084/etasr.3473.

[17]   H. Peng, J. Li, L. Löwenstein, and K. Hameyer, "A scalable, causal, adaptive energy management strategy based on optimal control theory

for a fuel cell hybrid railway vehicle," *Applied Energy*, vol. 267, Jun. 2020, Art. no. 114987, https://doi.org/10.1016/j.apenergy.2020.114987.

[18] M. A. Biberci and M. B. Celik, "Dynamic Modeling and Simulation of a PEM Fuel Cell (PEMFC) during an Automotive Vehicle's Driving Cycle," *Engineering, Technology & Applied Science Research*, vol. 10, no. 3, pp. 5796–5802, Jun. 2020, https://doi.org/10.48084/etasr.3352.

[19] T. Zeng *et al.*, "Modelling and predicting energy consumption of a range extender fuel cell hybrid vehicle," *Energy*, vol. 165, pp. 187–197, Dec. 2018, https://doi.org/10.1016/j.energy.2018.09.086.

[20] R. Shirwani, S. Gulzar, M. Asim, M. Umair, and M. A. Al-Rashid, "Control of vehicular emission using innovative energy solutions comprising of hydrogen for transportation sector in Pakistan: A case study of Lahore City," *International Journal of Hydrogen Energy*, vol. 45, no. 32, pp. 16287–16297, Jun. 2020, https://doi.org/10.1016/j.ijhydene.2019.02.173.